Solid State Physics

Byungwoo Park

Department of Materials Science and Engineering
Seoul National University

http://bp.snu.ac.kr

Types of Crystal Binding

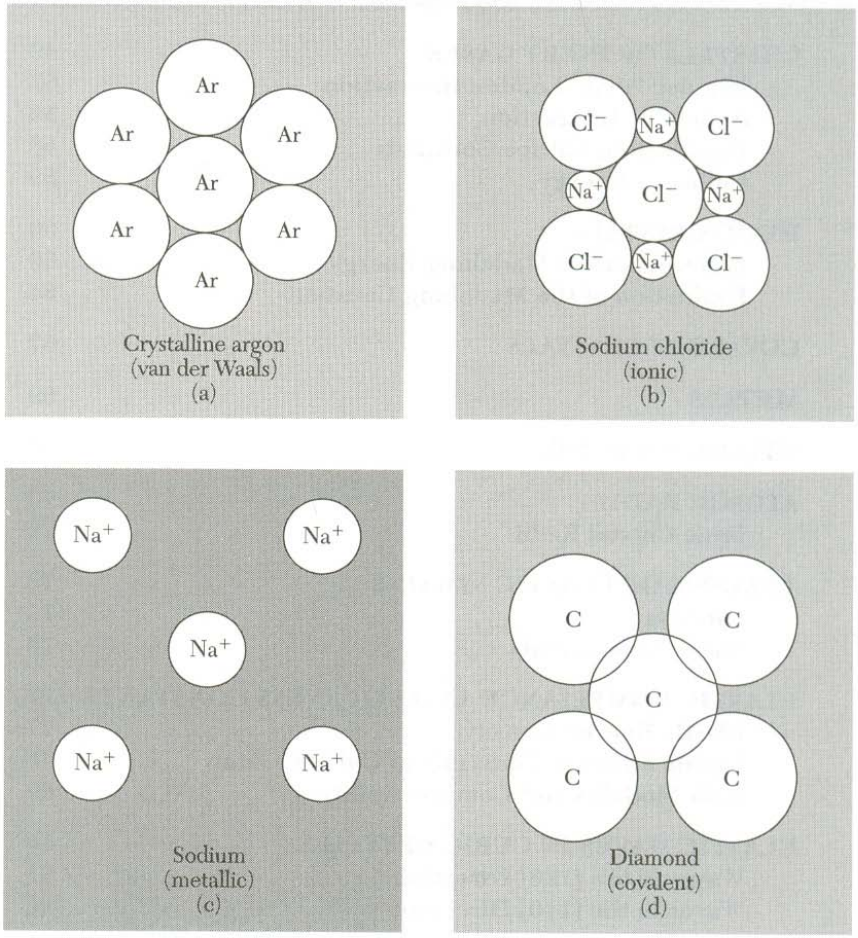

Figure 1 The principal types of crystalline binding. In (a) neutral atoms with closed electron shells are bound together weakly by the van der Waals forces associated with fluctuations in the charge distributions. In (b) electrons are transferred from the alkali atoms to the halogen atoms, and the resulting ions are held together by attractive electrostatic forces between the positive and negative ions. In (c) the valence electrons are taken away from each alkali atom to form a communal electron sea in which the positive ions are dispersed. In (d) the neutral atoms are bound together by the overlapping parts of their electron distributions.

Kittel, Solid State Physics (Chap. 3)

Cohesive Energies of Elements

See page 73

TABLE 1 Cohesive Energies of the Elements

Energy required to form separated neutral atoms in their ground electronic state from the solid at 0 K at 1 atm. The data were supplied by Prof. Leo Brewer in units kcal per mole, revised to February 20, 1975, after LBL report 3720.

Li	Be											B	C	N	O	F	Ne
158.	320.											556.	711.	474.	251.	81.0	1.92
1.63	3.32											5.77	7.37	4.92	2.60	0.84	0.020
37.7	76.5											133.	170.	113.4	60.03	19.37	0.46
Na	Mg											Al	Si	P	S	Cl	Ar
107.	145.											327.	446.	331.	275.	135.	7.74
1.113	1.51											3.39	4.63	3.43	2.85	1.40	0.080
25.67	34.7											78.1	106.7	79.16	65.75	32.2	1.85
K	Ca	Sc	Ti	V	Cr	Mn	Fe	Co	Ni	Cu	Zn	Ga	Ge	As	Se	Br	Kr
90.1	178.	37.6	468.	512.	395.	282.	413.	424.	428.	336.	130.	271.	372.	285.3	217.	118.	11.2
0.934	1.84	3.90	4.85	5.31	4.10	2.92	4.28	4.39	4.44	3.49	1.35	2.81	3.85	2.96	2.25	1.22	0.116
21.54	42.5	89.9	111.8	122.4	94.5	67.4	98.7	101.3	102.4	80.4	31.07	64.8	88.8	68.2	51.8	28.18	2.68
Rb	Sr	Y	Zr	Nb	Mo	Tc	Ru	Rh	Pd	Ag	Cd	In	Sn	Sb	Te	I	Xe
82.2	166.	422.	603.	730.	658.	661.	650.	554.	376.	284.	112.	243.	303.	265.	215.	107.	15.9
0.852	1.72	4.37	6.25	7.57	6.82	6.85	6.74	5.75	3.89	2.95	1.16	2.52	3.14	2.75	2.23	1.11	0.16
19.64	39.7	100.8	144.2	174.5	173.3	158.	155.4	132.5	89.8	68.0	26.73	58.1	72.4	63.4	51.4	25.62	3.80
Cs	Ba	La	Hf	Ta	W	Re	Os	Ir	Pt	Au	Hg	Tl	Pb	Bi	Po	At	Rn
77.6	183.	431.	621.	782.	859.	775.	788.	670.	564.	368.	65.	182.	196.	210.	144.		19.5
0.804	1.90	4.47	6.44	8.10	8.90	8.03	8.17	6.94	5.84	3.81	0.67	1.88	2.03	2.18	1.50		0.202
18.54	43.7	103.1	148.4	186.9	205.2	185.2	188.4	160.1	134.7	87.96	15.5	43.4	46.78	50.2	34.5		4.66
Fr	Ra	Ac															
	160.	410.															
	1.66	4.25															
	38.2	98.															

Ce	Pr	Nd	Pm	Sm	Eu	Gd	Tb	Dy	Ho	Er	Tm	Yb	Lu
417.	357.	328.		206.	179.	400.	391.	294.	302.	317.	233.	154.	428.
4.32	3.70	3.40		2.14	1.86	4.14	4.05	3.04	3.14	3.29	2.42	1.60	4.43
99.7	85.3	78.5		49.3	42.8	95.5	93.4	70.2	72.3	75.8	55.8	37.1	102.2
Th	Pa	U	Np	Pu	Am	Cm	Bk	Cf	Es	Fm	Md	No	Lr
598.		536.		347.	264.	372.							
6.20		5.55		3.60	2.73	3.86							
142.9		128.		83.0	63.	89.							

kJ/mol
eV/atom
kcal/mol

Kittel, Solid State Physics (Chap. 3)

Bond Energies for Single Covalent Bonds

TABLE 7 Energy Values for Single Covalent Bonds

Bond	Bond Energy eV	Bond Energy kJ/mol	Bond	Bond Energy eV	Bond Energy kJ/mol
H—H	4.5	435	P—P	2.2	213
C—C	3.6	347	O—O	1.4	138
Si—Si	1.8	176	Te—Te	1.4	138
Ge—Ge	1.6	159	Cl—Cl	2.5	243

After L. Pauling.

W. Luft Y.S. Tsuo (1993)
"Hydrogenated Amorphous Silicon Alloy Deposition Process"
P.14

Si-H 3.4eV
Si-Si: 2.2eV

Kittel, Solid State Physics (Chap. 3)

Bond Energy – Lange's Handbook of Chemistry

Bonding Energy (eV)	Bond		Bonding Energy (eV)	Bond		Bonding Energy (eV)	Bond		Bonding Energy (eV)	Bond		Bonding Energy (eV)
1,927	Cerium	Ce–Ce	2,518	Hafnium	Hf–C	5,679	Nickel	Ni–Ni	2,715	Sodium	Na–Na	0,798
2,642		Ce–N	5,378		Hf–N	5,534		Ni–Cl	3,855		Na–Cl	4,249
5,119		Ce–O	8,238		Hf–O	8,197		Ni–F	4,508		Na–H	2,083
2,238		Ce–S	5,938	Hydrogen	H–H	4,518		Ni–H	2,995		Na–K	0,659
2,953	Cesium	Cs–Cl	4,55		H–C	3,492		Ni–O	4,058		Na–O	2,663
1,824		Cs–O	3,078		H–C≡CH	5,42		Ni–S	3,731		Na–OH	3,948
3,078	Chlorine	Cl–Cl	2,514		H–CH=CH$_2$	4,425		Ni–Si	3,295	Sulfur	S–S	4,446
5,399		Cl–C	3,503		H–C$_6$H$_5$	4,466	Nitrogen	N–N	9,796		S–Cl	2,642
2,207		Cl–F	2,596		H–CN	5,596		N–Cl	4,031		S–F	3,554
3,876		Cl–N	4,031		H–Cl	4,475		N–F	3,119		S–N	4,808
2,601		Cl–O	2,819		H–CO	1,306		N≡N	9,803		S–O	5,409
3,959		Cl–P	2,995		H–CHO	3,772		N–O	6,534	Tin	Sn–Sn	2,021
4,642	Chromium	Cr–H	2,902		H–COOH	3,901		N–P	6,394		Sn–Cl	4,207
2,176		Cr–N	3,917		H–F	5,892		N–S	4,808		Sn–F	4,839
2,819		Cr–O	4,425		H–I	3,095	Oxygen	O–O	5,164		Sn–H	2,767
6,031	Cobalt	Co–Co	1,731		H–N	3,254		O–Cl	2,819		Sn–I	2,425
4,984		Co–Cu	1,679		H–N$_3$	3,689		O–F	2,301		Sn–O	5,679
5,534		Co–O	3,813		H–O	4,435		O–I	1,907		Sn–S	4,808
3,834		Co–S	3,554		H–OH	5,168		O–N	6,534	Tungsten	W–O	6,767
4,601	Copper	Cu–Cu	2,093		H–OCH$_3$	4,526		HO–OH	2,216		W–P	3,161
5,834		Cu–Cl	3,969		H–ONO	3,395		O–OH	2,777	Zinc	Zn–Zn	0,301
4,943		Cu–F	4,466		H–P	3,554	Phosphorus	P–P	5,078		Zn–Br	1,472
3,078		Cu–Ga	2,238		H–S	3,565		P–C	5,316		Zn–Cl	2,373
4,642		Cu–Ge	2,166		H–Si	3,093		P–H	3,554		Zn–F	3,813
4,031		Cu–H	2,902		H–SiH$_3$	4,073		P–N	6,394		Zn–H	0,889
8,352		Cu–I	2,041		H–Si(CH$_3$)$_3$	3,907		P–O	6,182		Zn–I	1,43
3,596		Cu–Ni	2,135	Indium	In–In	1,036		P–S	3,585		Zn–O	2,944
6,021		Cu–O	3,554		In–Cl	4,55		P=S	3,762		Zn–S	2,124
2,01		Cu–S	2,953		In–F	5,244	Platinum	Pt–B	4,953	Zirconium	Zr–C	5,813
2,902		Cu–Sn	1,834		In–O	3,731		Pt–H	3,648		Zr–F	6,456
2,269	Fluorine	F–F	1,627		In–P	2,051		Pt–O	3,596		Zr–N	5,855
2,425		F–N	3,119		In–S	2,995		Pt–P	4,321		Zr–O	7,876
2,86	Gallium	Ga–Ga	1,43	Iron	Fe–Fe	1,036		Pt–Si	5,192		Zr–S	5,959
2,435		Ga–O	2,953		Fe–Br	2,56	Potassium	K–K	0,594			
1,472		Ga–P	2,383		Fe–O	4,238		K–Cl	4,425			
2,031	Germanium	Ge–Ge	2,839		Fe–S	3,513		K–Na	0,659			
3,212		Ge–Cl	4,476		Fe–Si	3,078		K–O	2,477			
0,155		Ge–F	5,026	Lithium	Li–Li	1,098		K–OH	3,554			
1,739		Ge–H	3,326		Li–Br	4,383	Silicon	Si–Si	3,389			
4,808		Ge–O	6,86		Li–Cl	4,86		Si–Br	3,554			
6,29		Ge–S	5,71		Li–F	5,979		Si–C	4,508			
3,813		Ge–Si	3,119		Li–H	2,56		Si–Cl	4,725			
7,067	Gold	Au–Au	2,29		Li–I	3,648		Si–F	5,596			
9,969		Au–B	3,813		Li–Na	0,912		Si–H	3,098			
6,249		Au–Cl	3,554		Li–O	3,534		Si–I	3,513			
4,114		Au–Cu	2,404		Li–OH	4,425		Si–N	4,549			
5,554		Au–Fe	1,937	Magnesium	Mg–Mg	0,083		Si–O	8,269			
3,492		Au–Ga	3,047		Mg–Cl	3,295		Si–S	6,415			
2,166		Au–Ge	2,87		Mg–H	2,041	Silver	Ag–Ag	1,689			
7,98		Au–H	3,254		Mg–O	4,083		Ag–Au	2,104			
9,71		Au–Li	0,705		Mg–S	3,212		Ag–Cu	1,824			
1,254		Au–Mg	2,518	Manganese	Mn–Cl	3,741		Ag–Ga	1,865			
11,155		Au–Mn	1,917		Mn–Cu	1,648		Ag–Ge	1,813			
3,472		Au–Ni	2,839		Mn–O	4,166		Ag–H	2,342			
3,212		Au–Si	3,233		Mn–S	3,119		Ag–O	2,207			
6,031		Au–Sn	0,528		Mn–Se	2,083		Ag–Sn	1,409			

Fractional Ionic Character of Bonds in Binary Crystals

TABLE 8 Fractional Ionic Character of Bonds in Binary Crystals

Crystal	Fractional Ionic Character	Crystal	Fractional Ionic Character
Si	0.00		
SiC	0.18	CuCl	0.75
Ge	0.00	CuBr	0.74
ZnO	0.62	AgCl	0.86
ZnS	0.62	AgBr	0.85
ZnSe	0.63	AgI	0.77
ZnTe	0.61		
		MgO	0.84
CdO	0.79	MgS	0.79
CdS	0.69	MgSe	0.79
CdSe	0.70		
CdTe	0.67	LiF	0.92
		NaCl	0.94
InP	0.42	RbF	0.96
InAs	0.36		
InSb	0.32		
GaAs	0.31		
GaSb	0.26		

After J. C. Phillips, *Bonds and bands in semiconductors*, Academic Press, 1973, Chap. 2.

Kittel, Solid State Physics (Chap. 3)

Optical Phonon vs. Acoustical Phonon

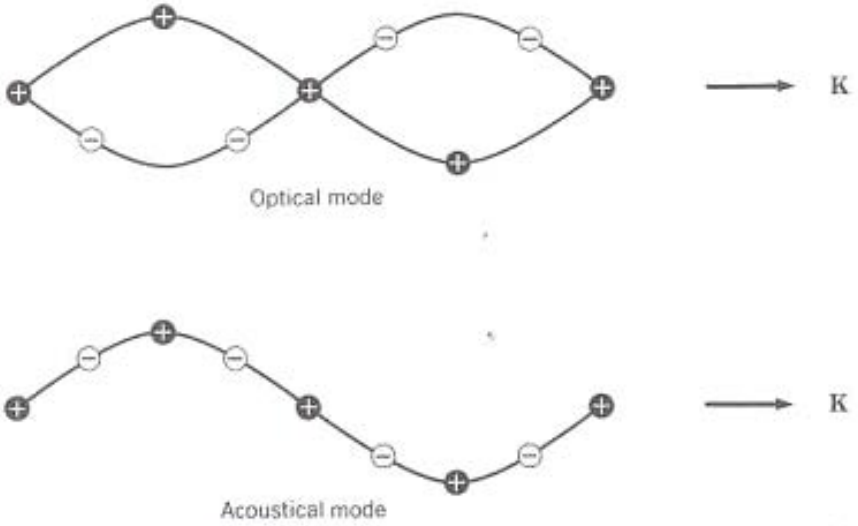

Figure 10 Transverse optical and transverse acoustical waves in a diatomic linear lattice, illustrated by the particle displacements for the two modes at the same wavelength.

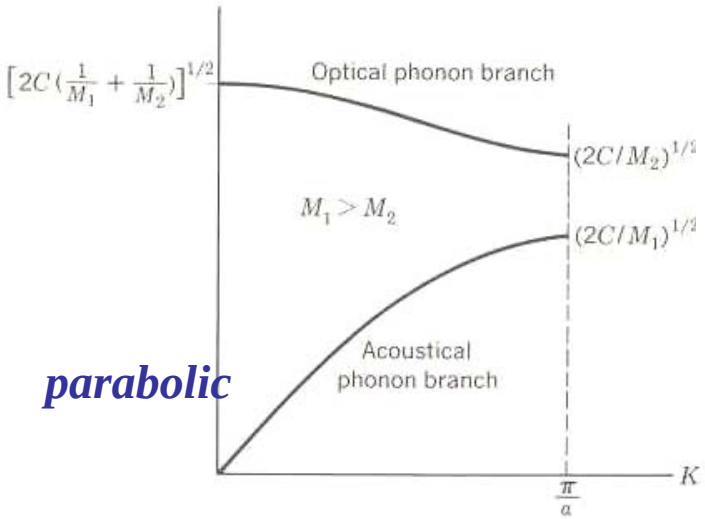

parabolic

Figure 7 Optical and acoustical branches of the dispersion relation for a diatomic linear lattice, showing the limiting frequencies at $K = 0$ and $K = K_{max} = \pi/a$. The lattice constant is a.

Kittel, Solid State Physics (Chap. 4)

Phonon: Density of State

Density of State for Phonon:

- The vibrations of the lattice (heat)
- Given frequency (energy), possible phonon mode
- Heat capacity

$$U = \int d\omega\, D(\omega)\langle n(\omega)\rangle \hbar\omega$$

***D*(*w*): density of state**
<*n*> : Plank distribution
$C_v = (\delta U/\delta T)_v$

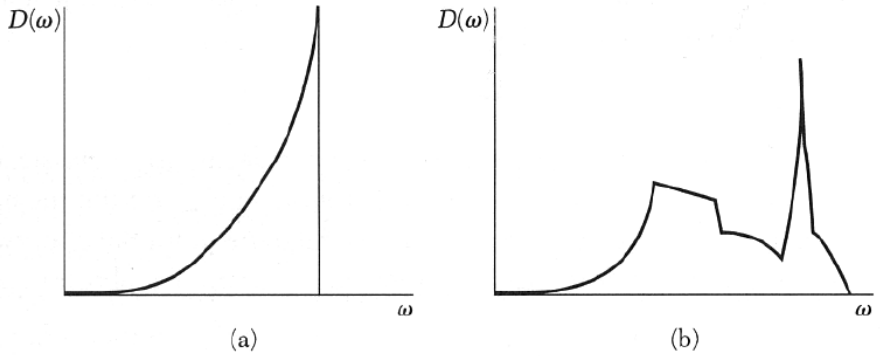

Figure 14 Density of states as a function of frequency for (a) the Debye solid and (b) an actual crystal structure. The spectrum for the crystal starts as ω^2 for small ω, but discontinuities develop at singular points.

Debye Frequency / Debye Temperature

Kittel, Solid State Physics (Chap. 5)

Heat Capacity

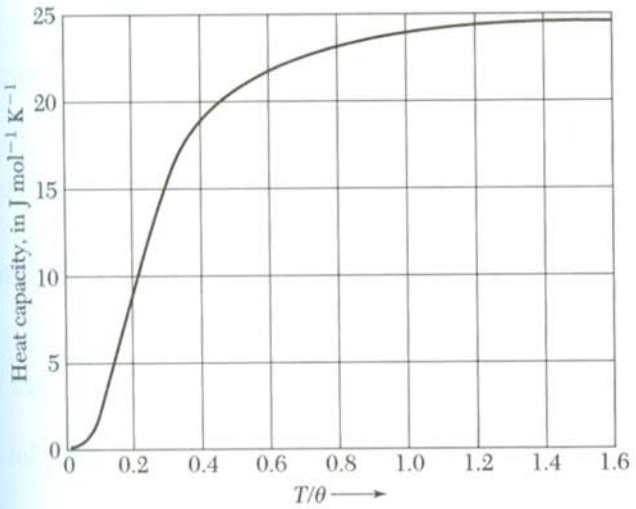

Debye Approximation

Figure 7 Heat capacity C_V of a solid, according to the Debye approximation. The vertical scale is in J mol^{-1} K^{-1}. The horizontal scale is the temperature normalized to the Debye temperature θ. The region of the T^3 law is below 0.1θ. The asymptotic value at high values of T/θ is 24.943 J mol^{-1} deg^{-1}.

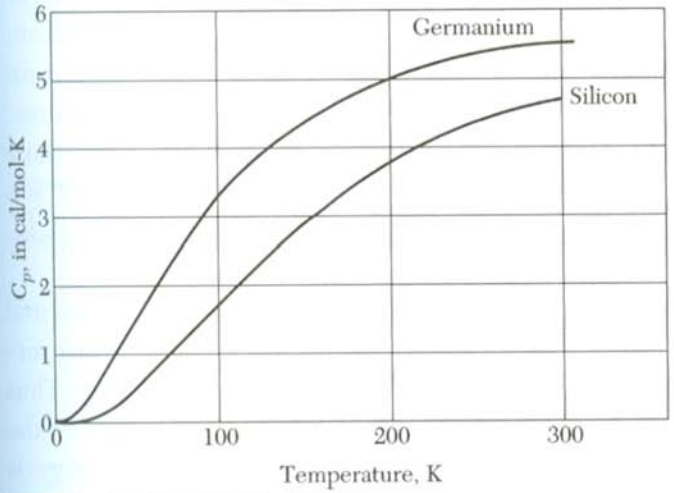

Heat Capacity

Figure 8 Heat capacity of silicon and germanium. Note the decrease at low temperatures. To convert a value in cal/mol-K to J/mol-K, multiply by 4.186.

Kittel, Solid State Physics (Chap. 5)

Density of Occupied State for Electrons

$E = (\hbar k)^2/2m$ $\quad k = (3\pi^2 n/V)^{1/3}$

$D(E) = dn/dE = V/2\pi^2(2m/\hbar)^{3/2}E^{1/2}$

Density of occupied state = $D(E)f(E)$

$= 1/[\exp\{(E-E_F)/kT\}+1]\ V/2\pi^2(2m/\hbar)^{3/2}E^{1/2}$

$DOS(E) = D(E) \sim E^{1/2}$

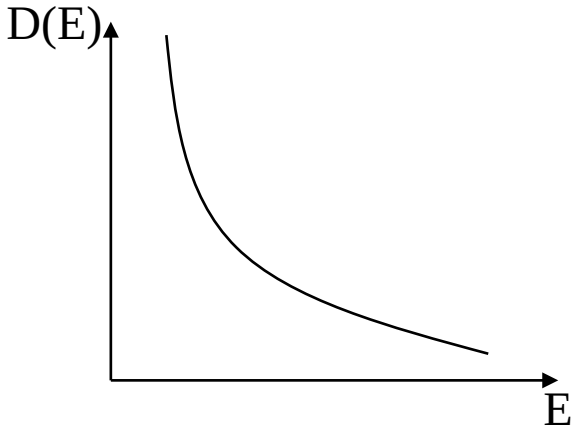

1-dimension

3-dimension

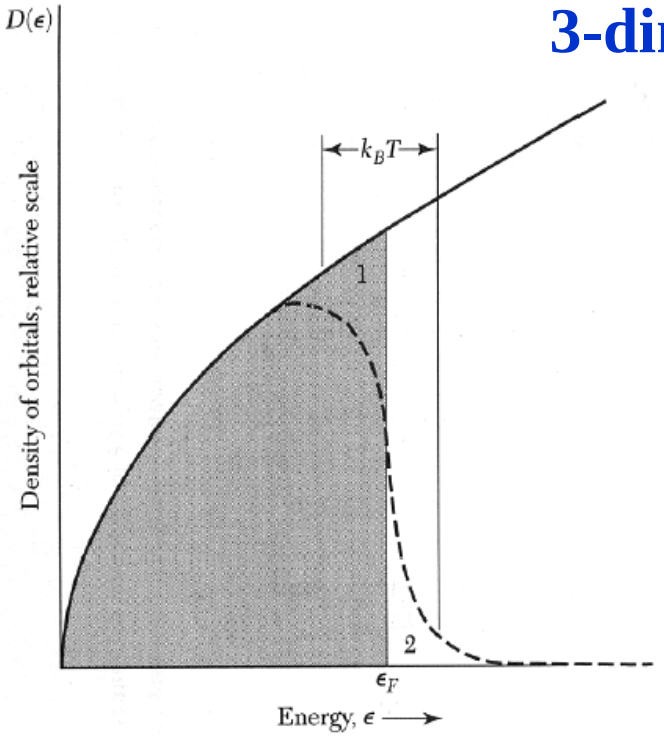

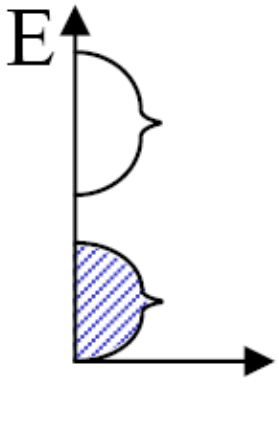

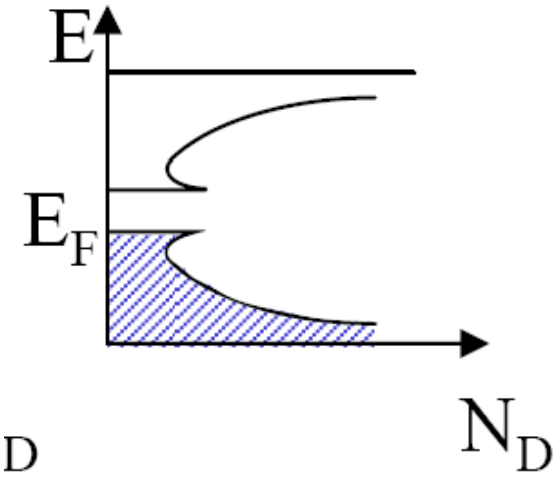

Kittel, Solid State Physics (Chap. 6)

Electrical Conductivity

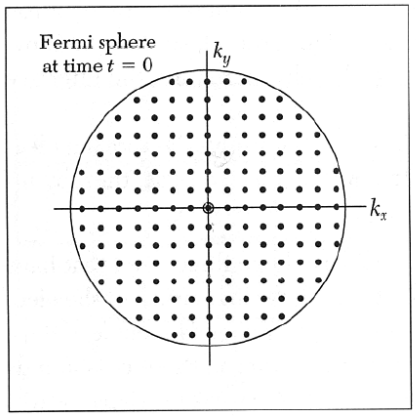

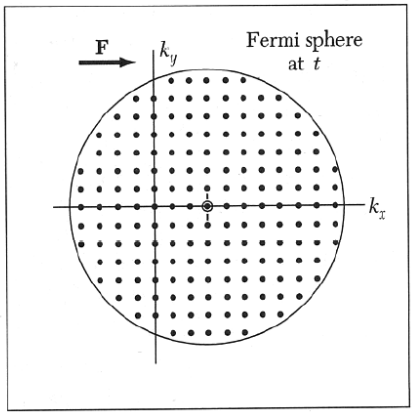

K(t)-k(0) = -eEt/ħ ; B = 0

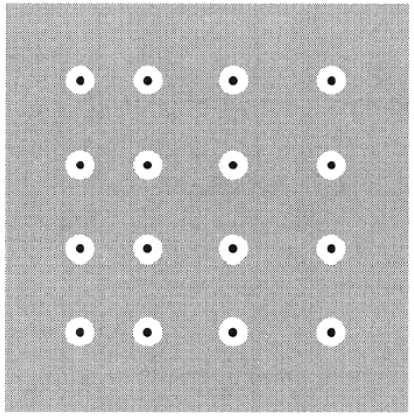

Phonon

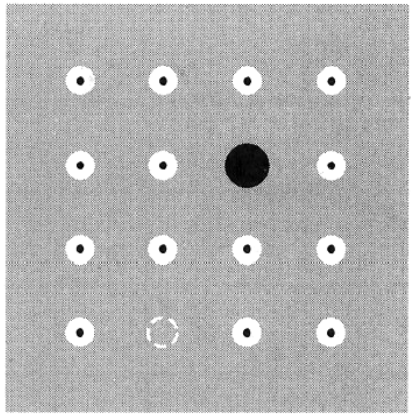

Impurity or Vacancy

Electrical conductivity: $\sigma = ne^2\tau/m$

$= ne\mu$

τ: collision time

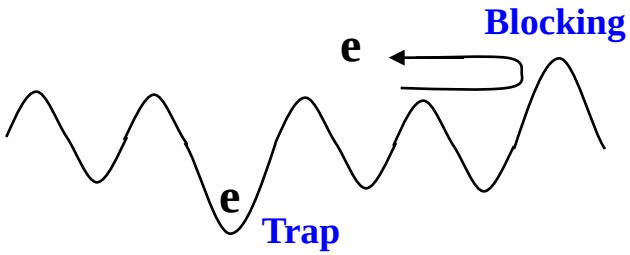

At 300 K, lattice phonon
At 4 K, imperfection

Au 4.55 (ohm·cm)$^{-1}$ **Pt 0.96 (ohm·cm)$^{-1}$**
Ru 1.35 (ohm·cm)$^{-1}$ **Al 3.65 (ohm·cm)$^{-1}$**

Kittel, Solid State Physics (Chap. 6)

Electron-Electron Collision: Negligible

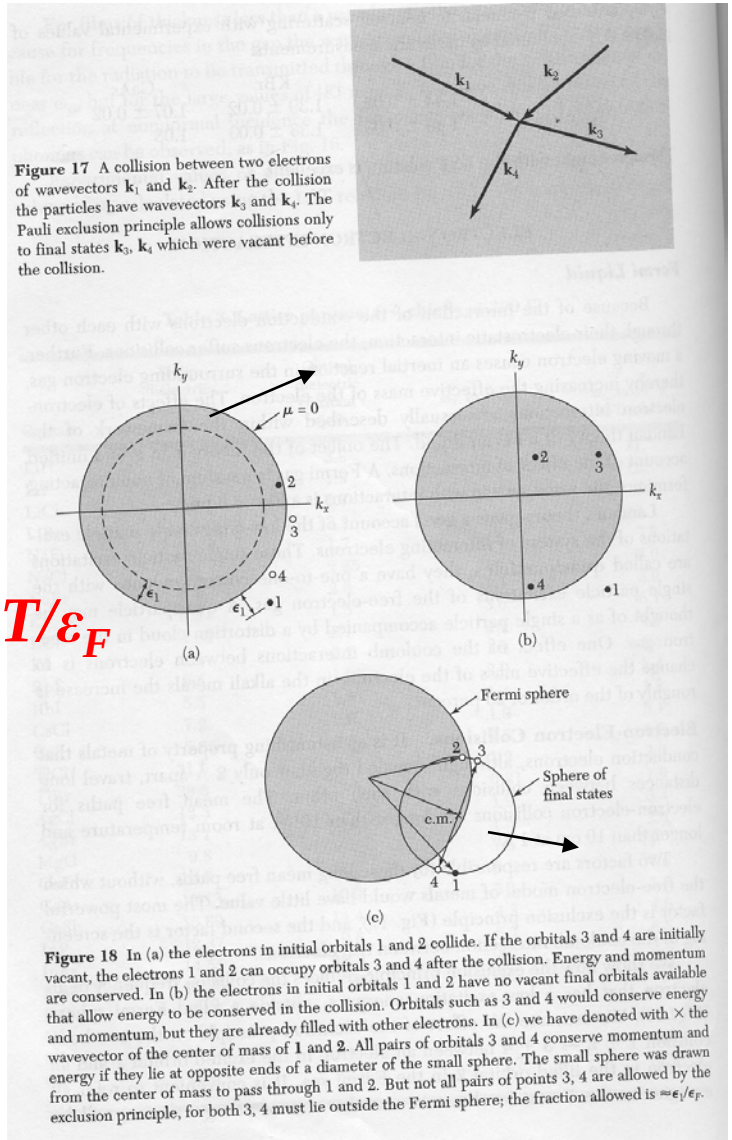

Figure 17 A collision between two electrons of wavevectors $\mathbf{k}_1$ and $\mathbf{k}_2$. After the collision the particles have wavevectors $\mathbf{k}_3$ and $\mathbf{k}_4$. The Pauli exclusion principle allows collisions only to final states $\mathbf{k}_3$, $\mathbf{k}_4$ which were vacant before the collision.

Figure 18 In (a) the electrons in initial orbitals 1 and 2 collide. If the orbitals 3 and 4 are initially vacant, the electrons 1 and 2 can occupy orbitals 3 and 4 after the collision. Energy and momentum are conserved. In (b) the electrons in initial orbitals 1 and 2 have no vacant final orbitals available that allow energy to be conserved in the collision. Orbitals such as 3 and 4 would conserve energy and momentum, but they are already filled with other electrons. In (c) we have denoted with × the wavevector of the center of mass of **1** and **2**. All pairs of orbitals 3 and 4 conserve momentum and energy if they lie at opposite ends of a diameter of the small sphere. The small sphere was drawn from the center of mass to pass through 1 and 2. But not all pairs of points 3, 4 are allowed by the exclusion principle, for both 3, 4 must lie outside the Fermi sphere; the fraction allowed is $\approx \epsilon_1/\epsilon_F$.

$\sim k_B T/\varepsilon_F$

Conduction electrons, although crowded together by only 2 Å, travel long distances between collisions.

→ why?

Conservation of energy

+

Conservation of momentum

The mean free path for electron-electron collisions is much longer than the mean free path for electron-phonon collisions at ~300 K.

Kittel, Solid State Physics (Chap. 14)

Electronic Structure of $AlPO_4$: Band Structure

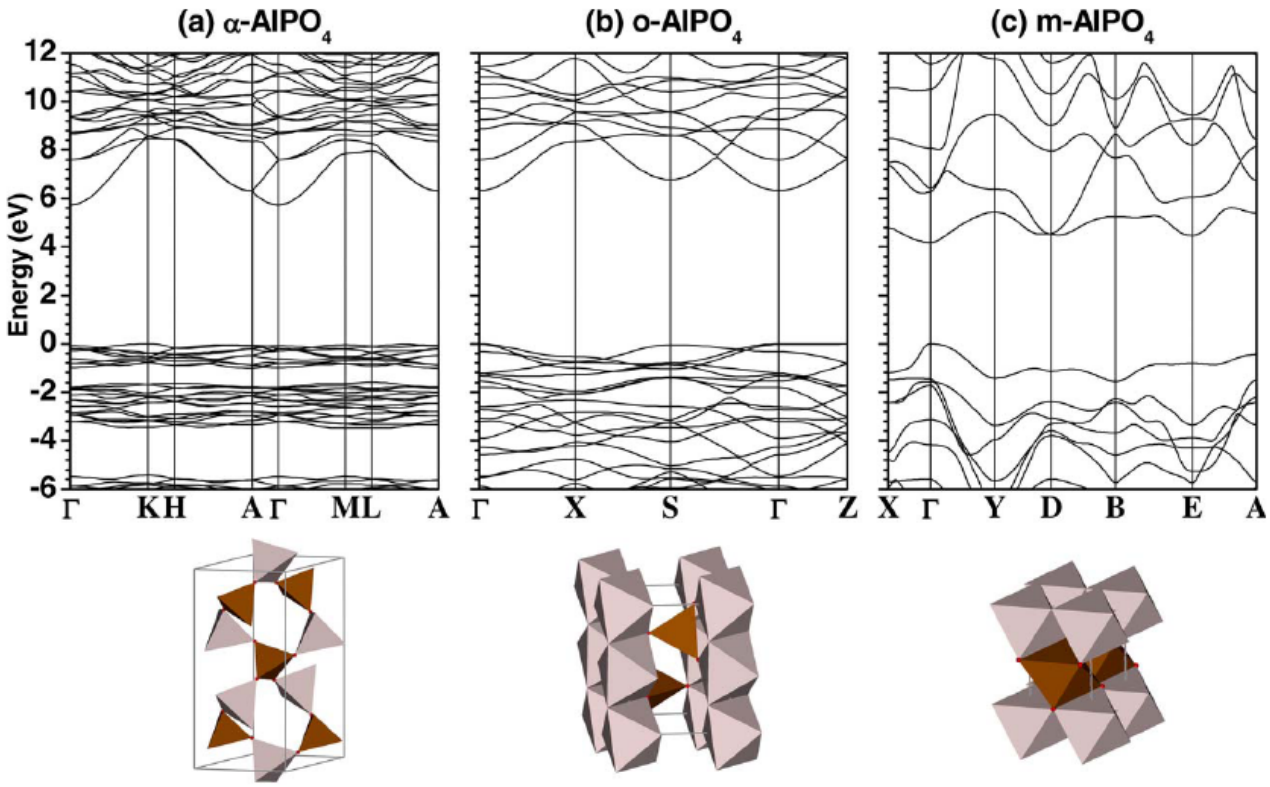

Fermi level

FIG. 1. (Color online) Band structures of (a) α, (b) o, and (c) m phases of $AlPO_4$. Also shown are the ball and stick sketches of the crystals showing the octahedral or tetrahedral units of the cations.

Bandgap: 5.71 eV **Bandgap: 6.32 eV** **Bandgap: 4.01 eV**

- Structural transformation under pressure

W. Y. Ching and Paul Rulis, University of Missouri-Kansas City
Physical Review B (2008)

Electronic Structure of $AlPO_4$: Absorption

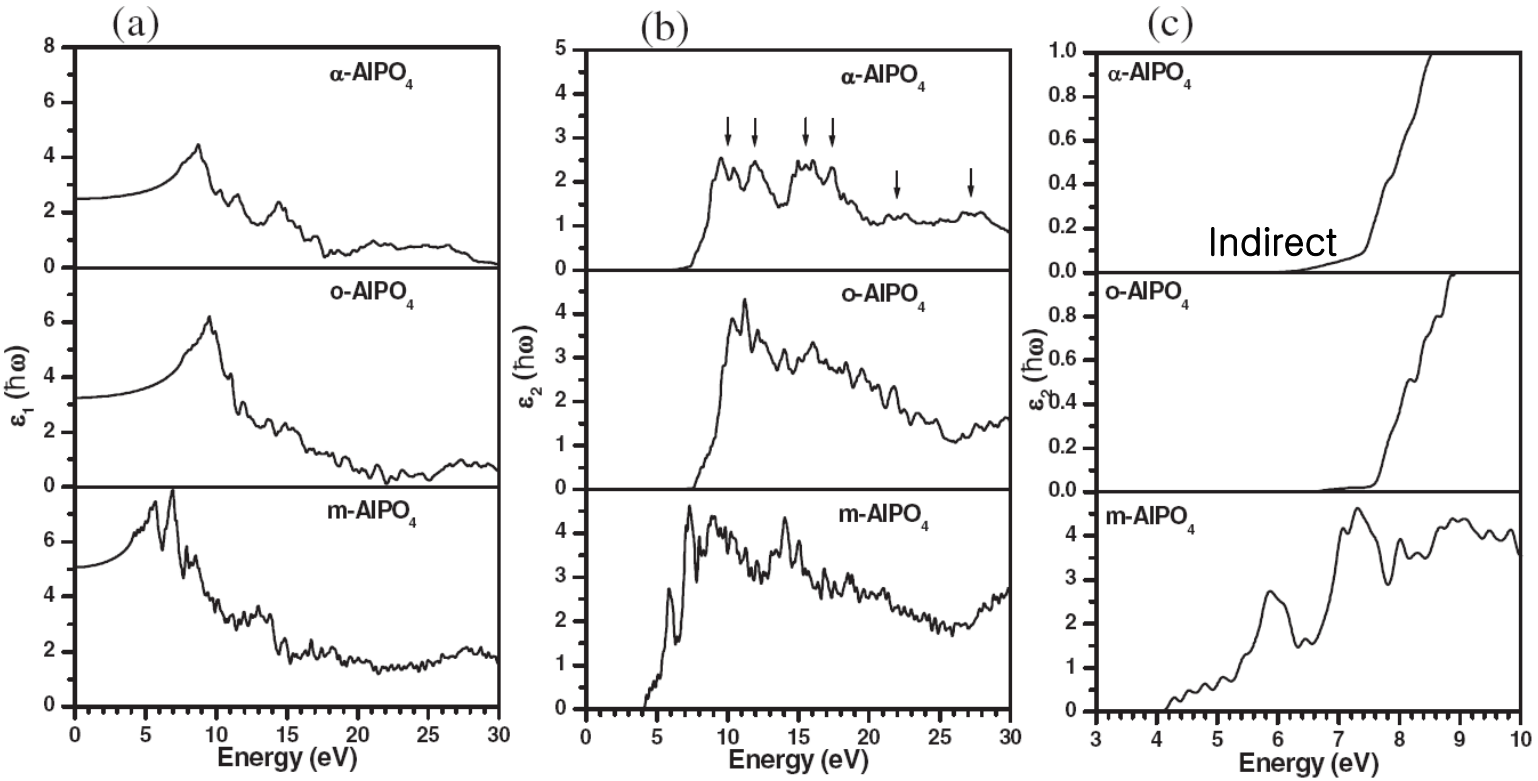

Real dielectric function **Imaginary dielectric function** **Absorption**

FIG. 4. Calculated (a) real and (b) imaginary parts of the complex dielectric functions for α-$AlPO_4$, o-$AlPO_4$, and m-$AlPO_4$. (c) The absorption near the onset in three crystals, showing the footlike structure for α-$AlPO_4$, o-$AlPO_4$.

W. Y. Ching and Paul Rulis, University of Missouri-Kansas City
Physical Review B (2008)

Transparent Conducting Oxide (TCO)

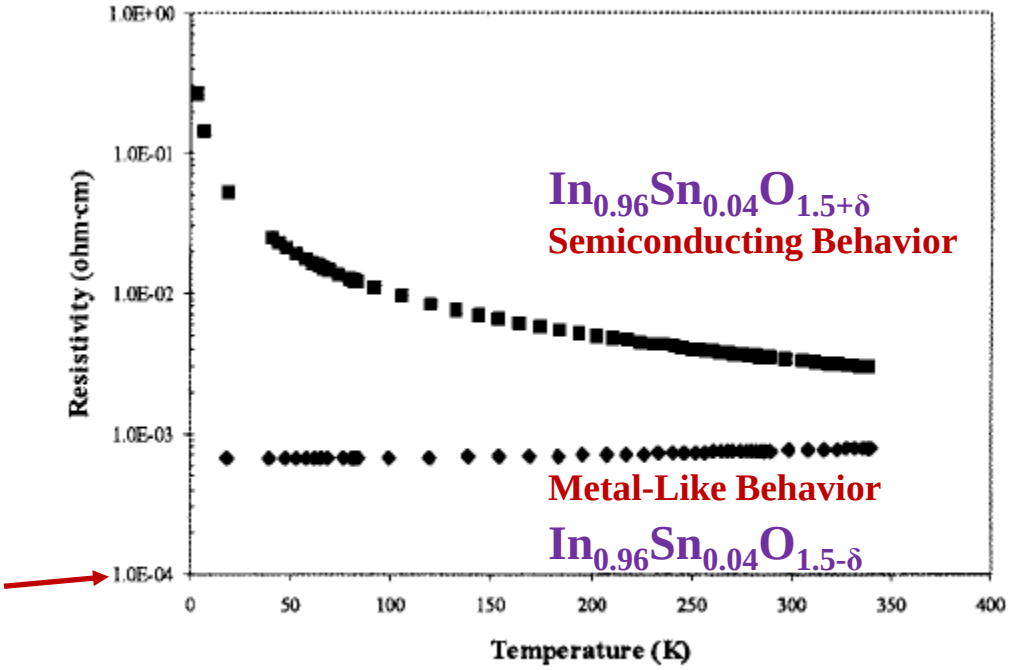

Figure 3. Low-temperature resistivity of as-fired (■) and reduced (♦) ITO.

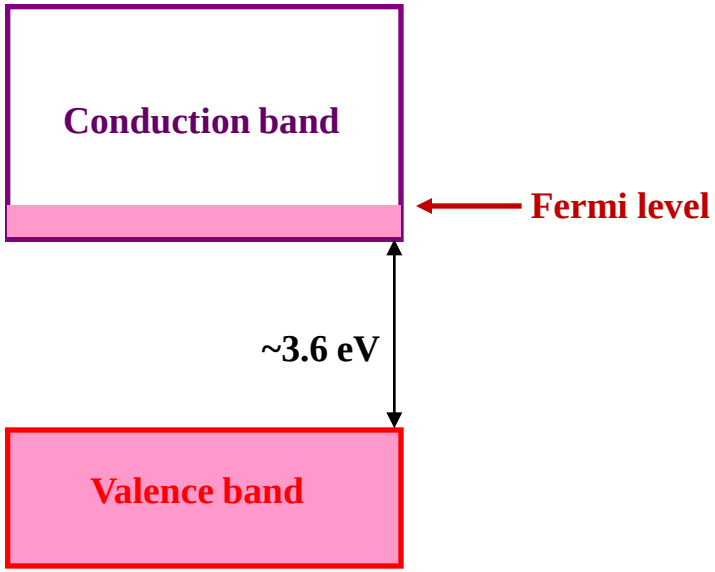

Reduction process (7% H_2 / 93% N_2): Removal of excess oxygen

K. R. Poeppelmeier's Group, Northwestern University
Chem. Mater. (2002)

Energy Levels of Free Electron in a 1-D Box

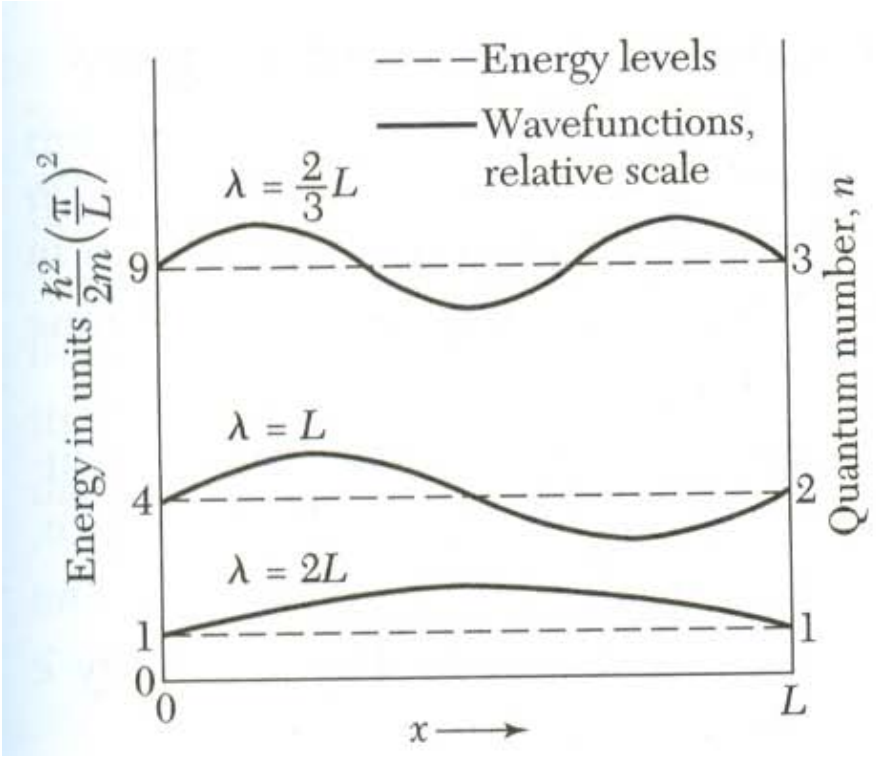

Figure 2 First three energy levels and wavefunctions of a free electron of mass m confined to a line of length L. The energy levels are labeled according to the quantum number n which gives the number of half-wavelengths in the wavefunction. The wavelengths are indicated on the wavefunctions. The energy ϵ_n of the level of quantum number n is equal to $(h^2/2m)(n/2L)^2$.

Kittel, Solid State Physics (Chap. 6)

Excitons in Nanoscale Systems

Box 1: An introduction to excitons in nanoscale systems

1. Bands and molecular orbitals for extended systems
Periodic, strongly coupled molecular or atomic systems are characterized by a high density of delocalized orbitals that form the valence (VB) and conduction (CB) bands. Those bands can be represented in real space as shown on the left side of the diagram, or equivalently, the energy of each band can be plotted against its wave vector k, as in the right schematic. Excitation of an electron from VB to CB creates free carriers. The minimum energy required is that of the bandgap, E_g.

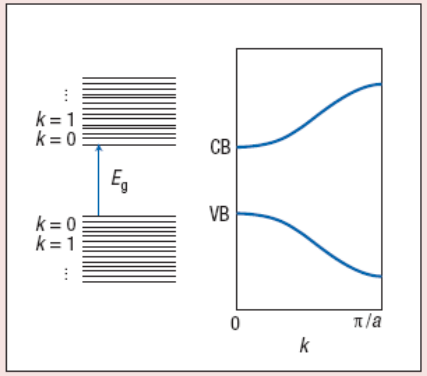

2. Excitons in extended systems: bound electron–hole pairs
The language that describes the features of the quasi-particle approach is nicely intuitive. An exciton in a spatially entended system is described as a neutral excitation particle: an electron–hole pair. In an exciton the electron and hole are bound by the electron-hole Coulomb interaction. In the chemist's electron–electron language, the 'attraction' derives from decreased electron–electron repulsion integrals in the excited state configuration compared with the ground state, thus lowering the energy of that configuration relative to the continuum by the exciton binding energy, $E_b = E_g - E_x$. Related electron–hole exchange interactions mix the Hartree–Fock (single particle) configurations, so that the exciton states are finally obtained through a configuration interaction (CI-singles) calculation. Correct spin eigenstates can only be obtained by antisymmetrizing wavefunctions and mixing configurations through exchange interactions.

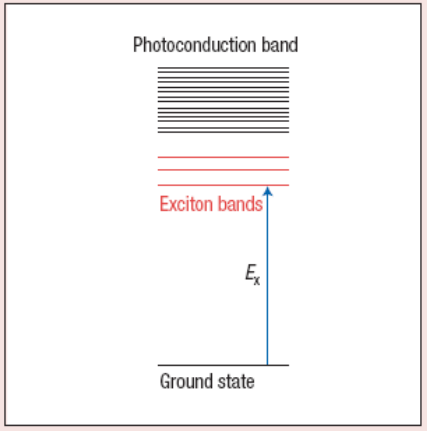

Si 14.7 meV
CdS 29.0 meV

Exciton Binding Energy

G. D. Scholes, Toronto University
Nat. Mater. (2006)

Quantum Confinement

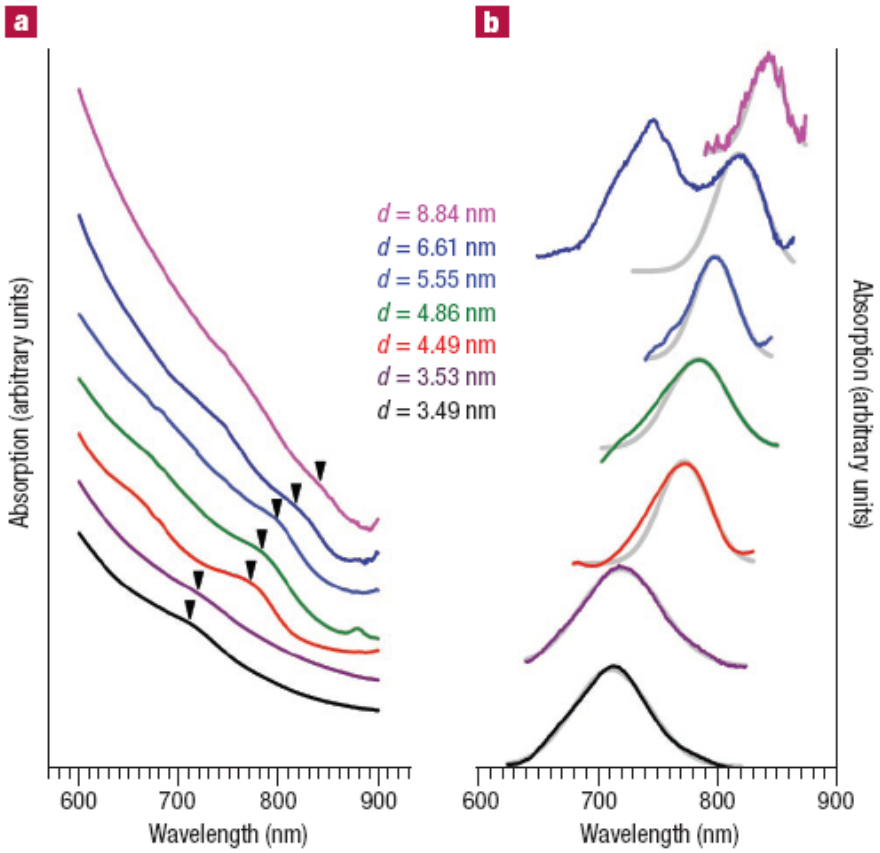

Figure 3 Spectral data. a, Absorption spectra from solutions of the InP quantum wires; arrowheads mark the lowest-energy excitonic absorptions. **b**, Excitonic peaks extracted by fitting and background subtraction (various colours), and the gaussian fits to those peaks (grey).

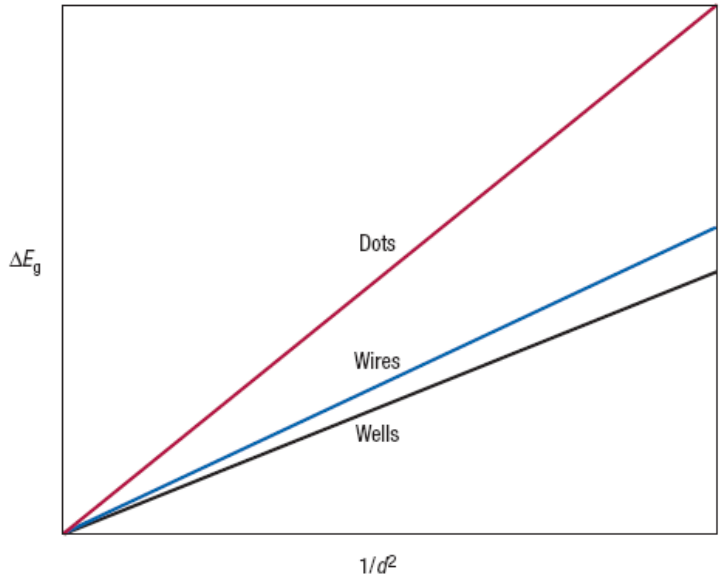

Figure 1 Predictions of simple particle-in-a-box models for the size dependences of the kinetic confinement energies of electrons and holes in corresponding quantum wells, wires and dots. The size parameter d refers to the thickness of a well, or the diameter of a wire or dot. The slopes of the lines are $(h^2/8)[1/m_e + 1/m_h]$ for the wells[9,10], $(1.17h^2/8)[1/m_e + 1/m_h]$ for the wires[11,12], and $(2h^2/8)[1/m_e + 1/m_h]$ for the dots[13], where h is Planck's constant, and m_e and m_h are the effective masses of an electron and hole, respectively.

W. E. Buhro, University of Washington
Nat. Mater. (2003)

Frequency Dependence of Polarizability

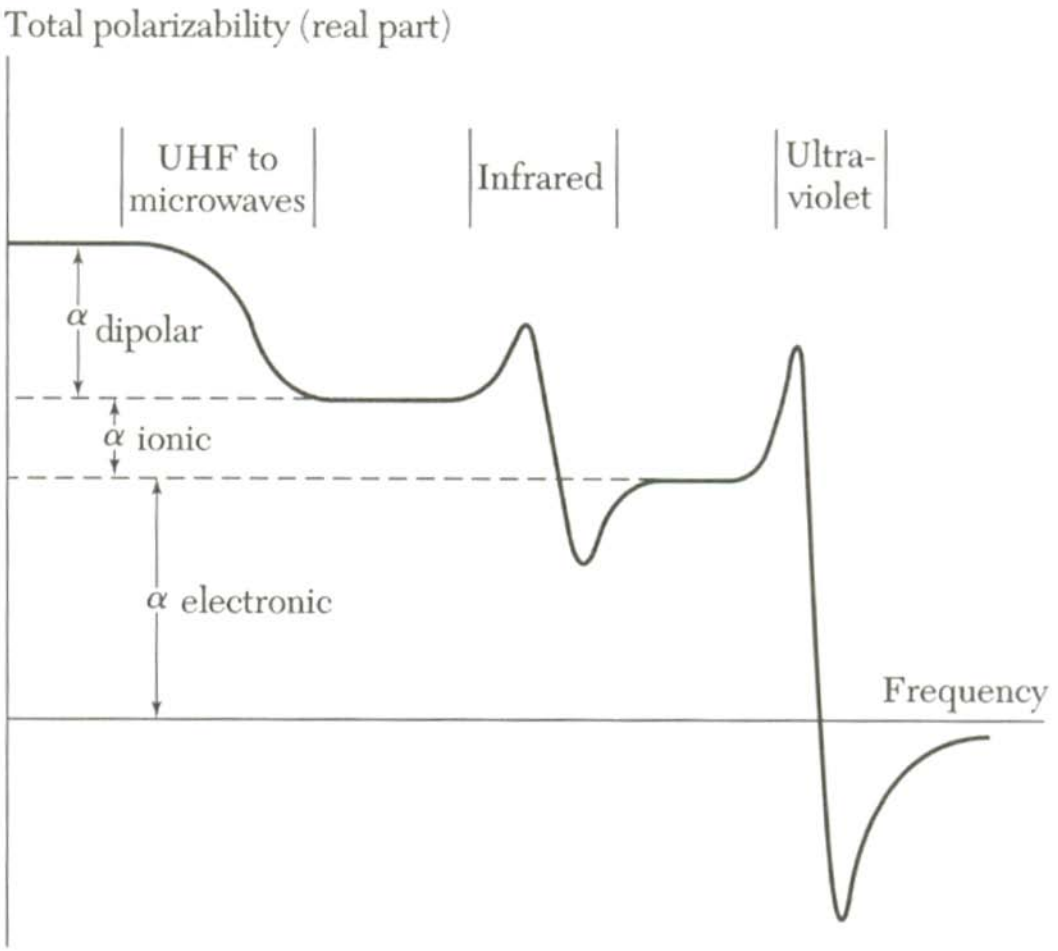

Figure 8 Frequency dependence of the several contributions to the polarizability.

Kittel, Solid State Physics (Chap. 16)

Dielectric Function of Free-Electron Gas (Plasmon)

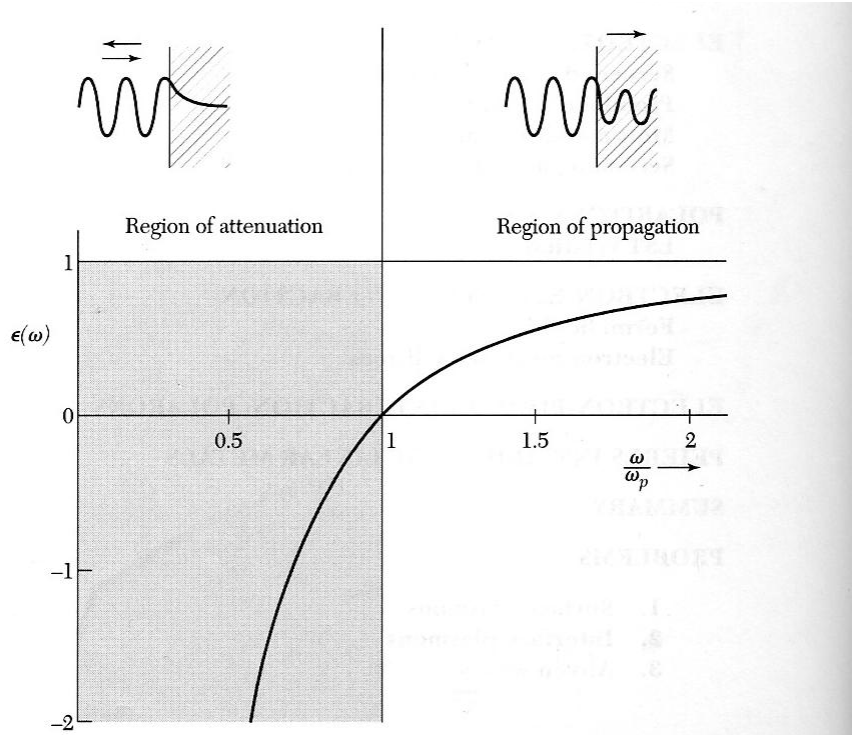

Figure 1 Dielectric function $\epsilon(\omega)$ or $\epsilon(\omega, 0)$ of a free-electron gas versus frequency in units of the plasma frequency ω_p. Electromagnetic waves propagate without damping only when ϵ is positive and real. Electromagnetic waves are totally reflected from the medium when ϵ is negative.

- Plasma: a medium with equal concentration of positive and negative charge, of which at least one charge type is mobile.

Motion of a free electron in an electric field

(assumption: long wavelength dielectric response, $e^{-i\omega t}$)

$$m\frac{d^2x}{dt^2} = -eE$$

$$\epsilon(\omega) = 1 - \frac{\omega_p^2}{\omega^2}\,, \quad \left(\ \omega_p^2 = 4\pi ne^2/m\ \right)$$

$\hbar\omega_p$ = 16 eV for Au

Kittel, Solid State Physics (Chap. 14)

Dispersion Relation for Transverse Electromagnetic Wave

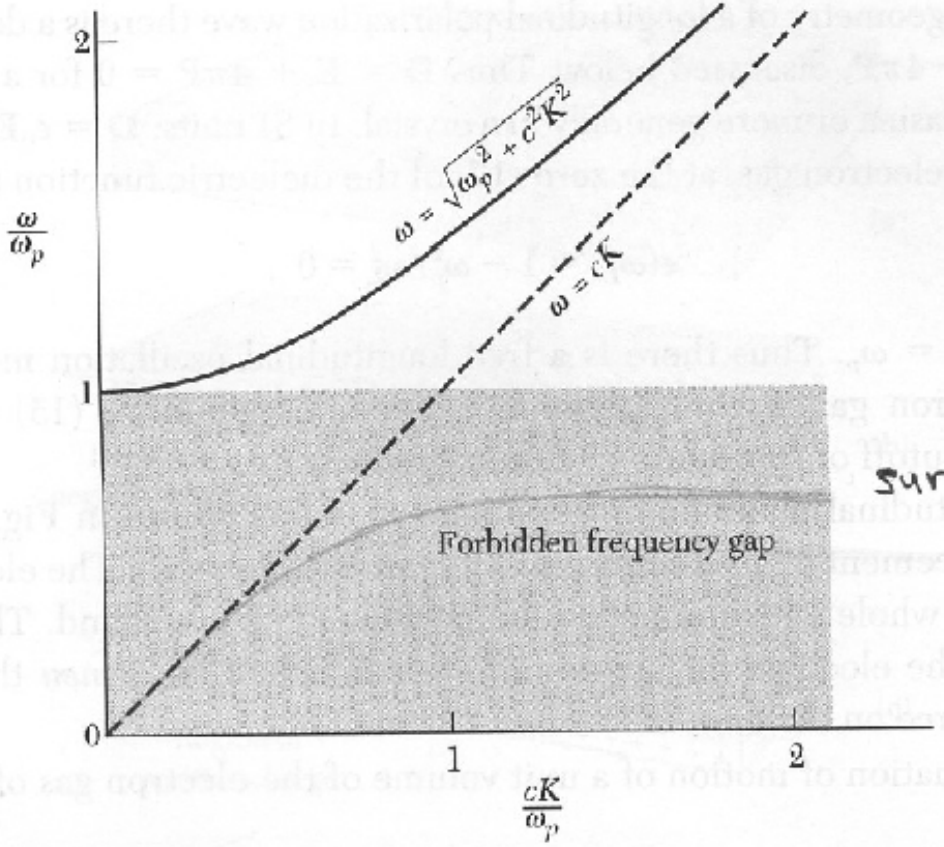

surface plasmons

$$k_{sp} = \frac{\omega}{c}\sqrt{\frac{\varepsilon_d \cdot \varepsilon_m}{\varepsilon_d + \varepsilon_m}}$$

Figure 2 Dispersion relation for transverse electromagnetic waves in a plasma. The group velocity $v_g = d\omega/dK$ is the slope of the dispersion curve. Although the dielectric function is between zero and one, the group velocity is less than the velocity of light in vacuum.

Kittel, Solid State Physics (Chap. 14)

Surface Plasmon of Nanoparticles

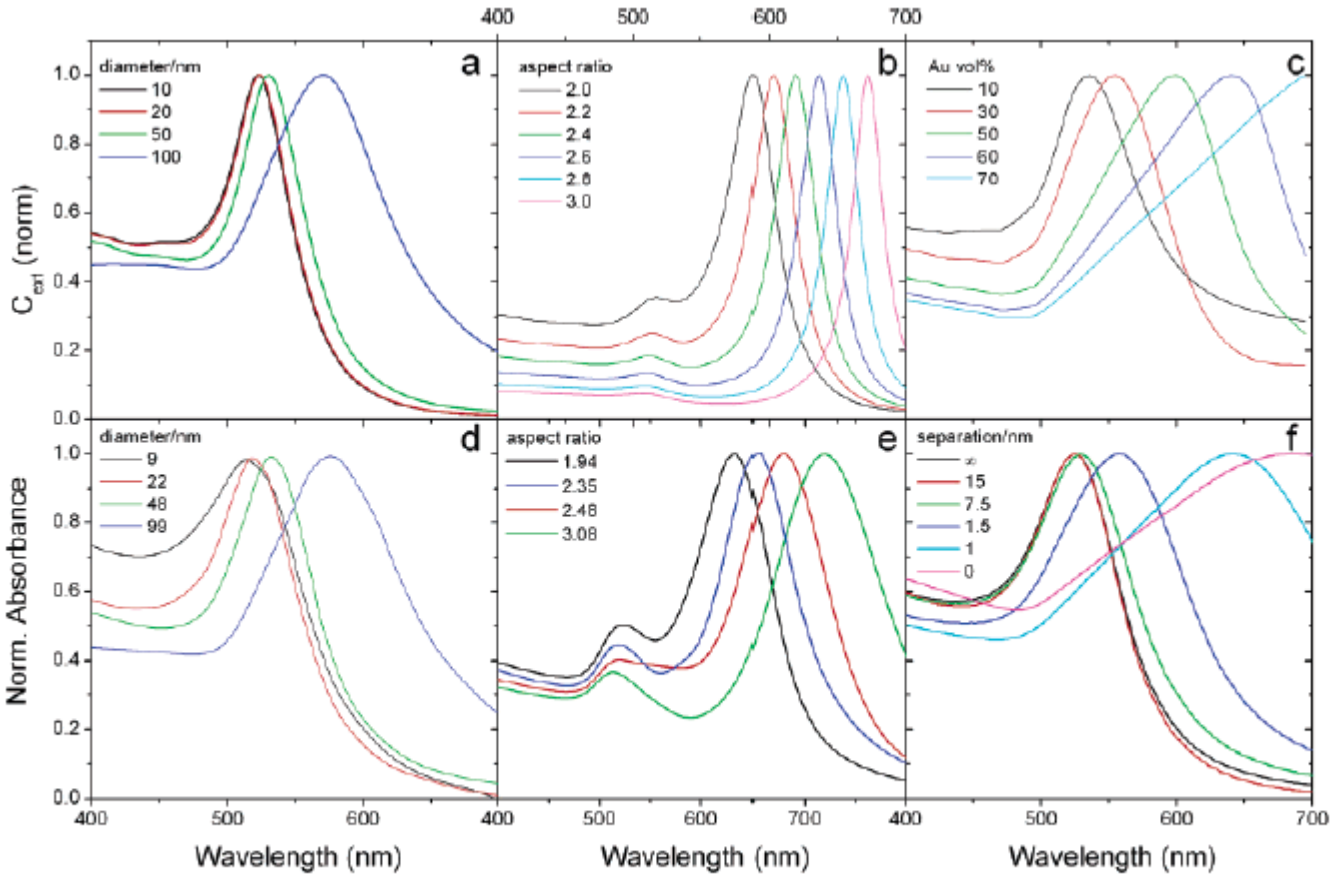

Figure 2. Top: Calculated UV−visible spectra for (a) Au spheres with varying diameters, (b) Au ellipsoids of varying aspect ratio, and (c) thin glass films loaded with increasing Au nanoparticle volume fractions. Bottom: Experimental spectra for (d) Au spheres,[40] (e) Au nanorods, and (f) multilayer films of glass-coated Au spheres with varying interparticle distance.

Luis M. Liz-Marzan, UniVersidade de Vigo, Langmuir (2006)

Surface Plasmon of Nanoparticles - Alloying

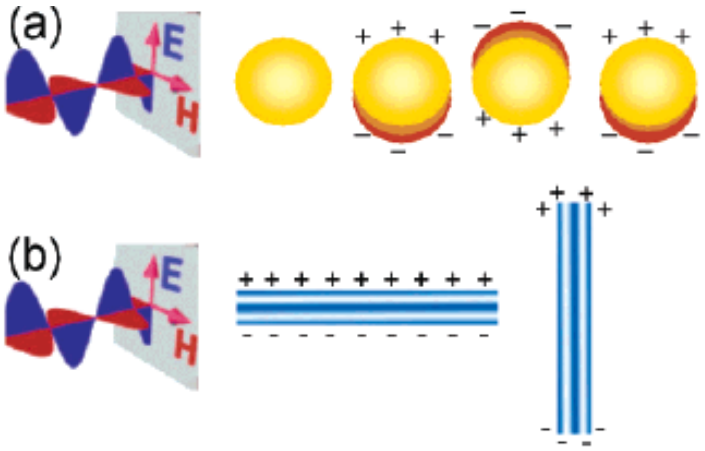

Figure 1. (a) Schematic drawing of the interaction of an electromagnetic radiation with a metal nanosphere. A dipole is induced, which oscillates in phase with the electric field of the incoming light. (b) Transversal and longitudinal oscillation of electrons in a metal nanorod.

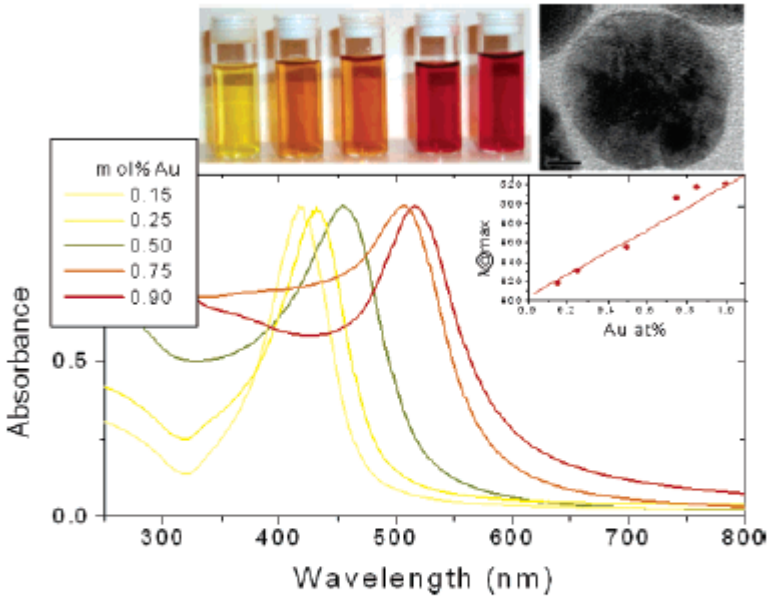

Figure 3. Variation in optical properties (UV−vis spectra and color) for AuAg alloy nanoparticle colloids with varying compositions. In the graph inset, the position of the experimental absorption band (dots) is plotted as a function of composition, and the solid line is a linear fit to values obtained using Mie theory. The HRTEM image shows the homogeneous distribution of Au and Ag atoms within the particles.

Luis M. Liz-Marzan
UniVersidade de Vigo, Langmuir (2006)

- The electric field of the incoming radiation induces the formation of a dipole in the nanoparticle, and there is a restoring force that tries to compensate it.
- Unique resonance frequency matches this electron oscillation within the nanoparticle.

- Tuning the surface-plasmon energy by alloying.

Surface-Plasmon Enhanced Photoluminescence

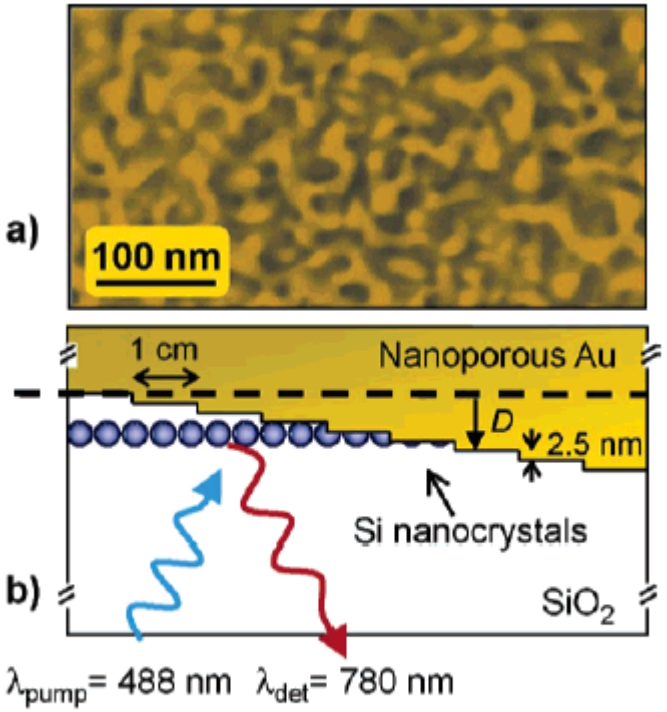

Figure 1. (a) False color plan view (100 K magnification) SEM of the nanoporous gold surface showing features on the order of 10 nm. (b) Schematic cross section of the sample. PL measurements are made from the bottom side of all samples.

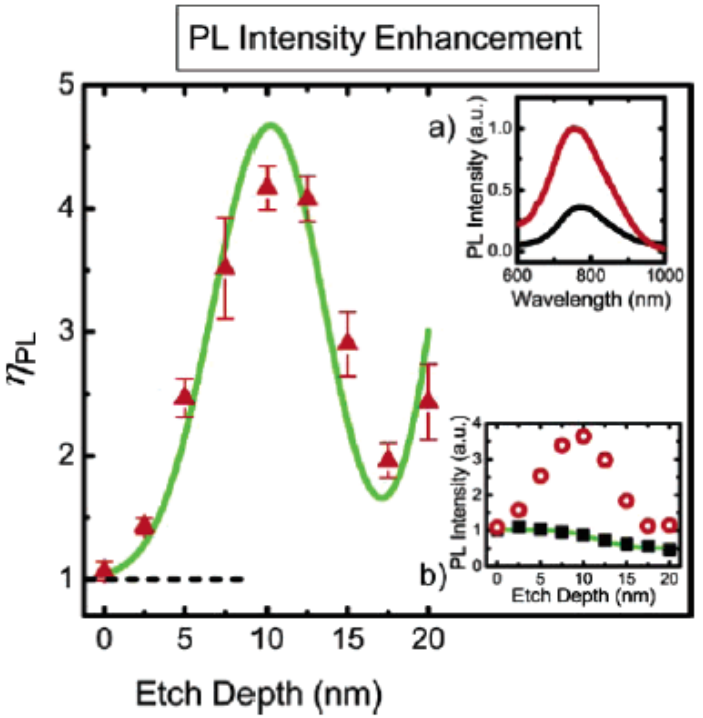

Figure 2. PL intensity enhancement, η_{PL}, measured at 780 nm as a function of etch depth, D (triangles). The solid line is a fit to the data using a model that accounts for the spatial distribution of Si nanocrystals and the enhanced local-field. Insets: (a) Typical PL spectra for the reference (black) and coupled np-Au/nc-Si (red) samples, at $D = 5$ nm. (b) PL intensities at 780 nm vs etch depth for the reference (squares) and coupled np-Au/nc-Si (circles) samples. The reference intensities are well fit by the green line, which is the integral of two Gaussian distributions that peak at 14.2 and 24.2 nm, respectively.

Prof. Harry Atwater, Caltech
Nano Lett. (2005)

Color of Metal

Metal의 color에 영향을 주는 요인

1. Free electron (bulk plasmon): Metal의 free electron oscillation에 의해 bulk plasmon 에너지보다 작은 에너지를 가지는 빛은 reflect 됨.
   대부분의 metal이 가시광 에너지보다 큰 bulk plasmon 에너지를 가지고 있기 때문에 reflect된 가시광으로 인해 기본적으로 금속광택을 띠게 됨.

2. Interband absorption: Metal이 빛과 interaction을 하려면
   같은 밴드내에서는 **momentum conservation**을 만족시키지 못하기 때문에,
   다른 band로의 electron transition이 일어나야 함.

   이때 일어날 수 있는 transition은 두가지 case가 있음:

   (1) Fermi level 근처의 conduction electron이 더 높은 위치에 있는 에너지 밴드로 이동
   (2) 아래쪽 레벨에 있는 밴드에 차있는 electron이 conduction band 쪽으로 이동

Ashcroft, Solid State Physics

Color of Metal – Cu Band Structure

Figure 15.11
Burdick's calculated bands for copper, illustrating that the absorption threshold for transitions up from the conduction band is about 4 eV, while the threshold for transitions from the *d*-band to the conduction band is only about 2 eV. (The energy scale is in tenths of a rydberg (0.1 Ry = 1.36 eV).) Note the resemblance of the bands other than the *d*-bands to the free electron bands plotted below.

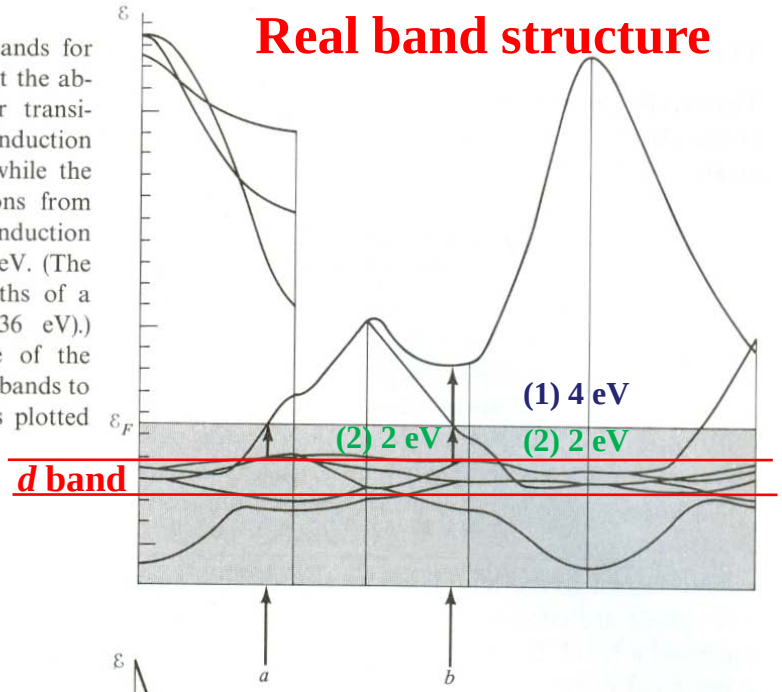

Free electron model

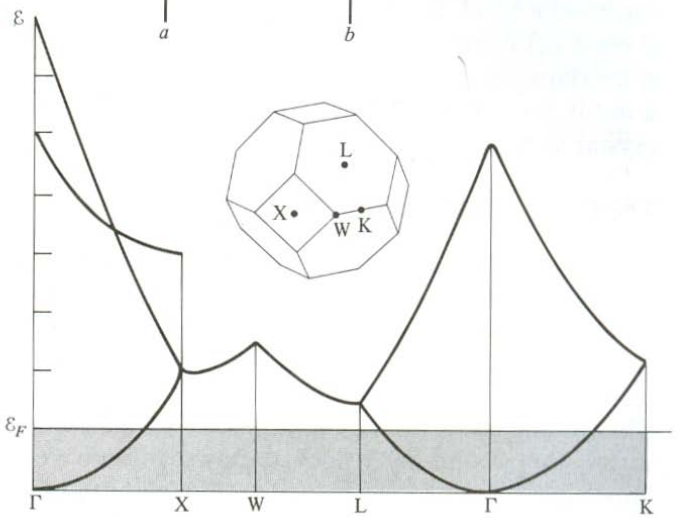

Fermi level 약간 아래쪽에 존재하는 Cu metal의 *d* band로 인해 아래쪽 그림에 없던 밴드들이 형성된 것을 확인할 수 있음.

Absorption이 일어날 수 있는 경우:

(1)의 경우 Fermi level 근처의 conduction electron이 더 높은 위치에 있는 에너지 밴드로 이동하는 것.

(2)의 경우 아래쪽 레벨에 있는 밴드에 차있는 electron이 conduction band 쪽으로 옮겨오는 것.

(2)의 경우가 에너지가 더 작으므로 2 eV 정도부터 흡수가 일어나게 됨.

Ashcroft, Solid State Physics

Color of Metal – Imaginary Dielectric Constant

아래 그림은 Cu와 Ag의 imaginary dielectric constant

- Cu 경우 윗장의 밴드구조에 의해 2 eV 부터 흡수가 일어나기 때문에 낮은 쪽 에너지의 색인 붉은 빛을 띠게 됨.
- Ag 경우 이러한 흡수가 4 eV 에서 일어나기 때문에 visible 영역에 영향을 주지 않아 투명한 광택색으로 보이게 됨.

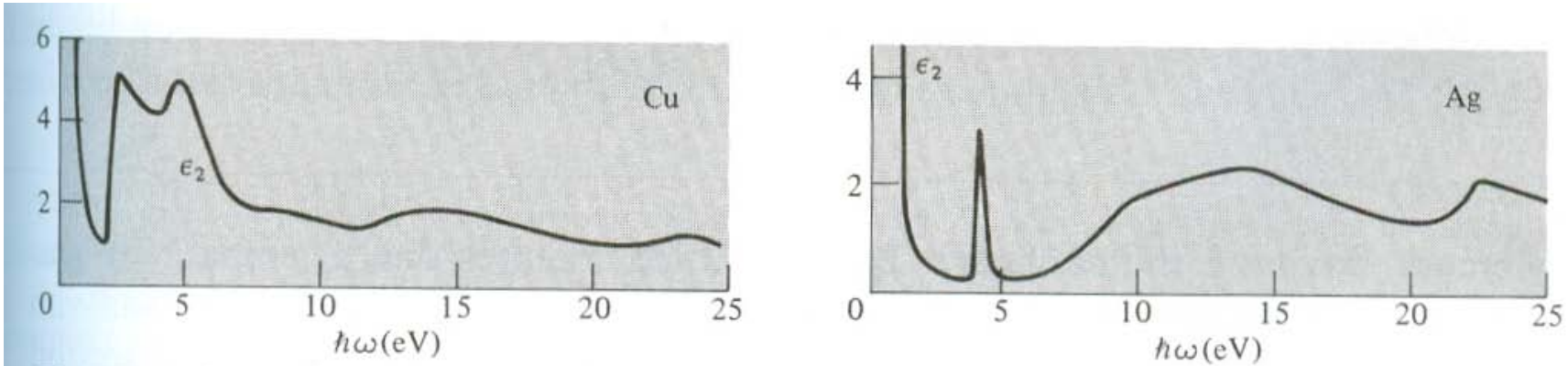

Figure 15.12
The imaginary part of the dielectric constant, $\epsilon_2(\omega) = \text{Im}\,\epsilon(\omega)$ vs. $\hbar\omega$, as deduced from reflectivity measurements. (H. Ehrenreich and H. R. Phillip, *Phys. Rev.* **128**, 1622 (1962).) Note the characteristic free electron behavior ($1/\omega^3$) below about 2 eV in copper and below about 4 eV in silver. The onset of interband absorption is quite apparent.

Ashcroft, Solid State Physics

Work Function

Table 2 Electron work functions[a]

7th Ed.

(Values obtained by photoemission, except tungsten obtained by field emission.)

Element	Surface plane	Work function, in eV
Ag	(100)	4.64
	(110)	4.52
	(111)	4.74
Cs	polycrystal	2.14
Cu	(100)	4.59
	(110)	4.48
	(111)	4.98
Ge	(111)	4.80
Ni	(100)	5.22
	(110)	5.04
	(111)	5.35
W	(100)	4.63
	(110)	5.25
	(111)	4.47

[a]After H. D. Hagstrum

Kittel, Solid State Physics (Chap. 17)

Work Function (not real)

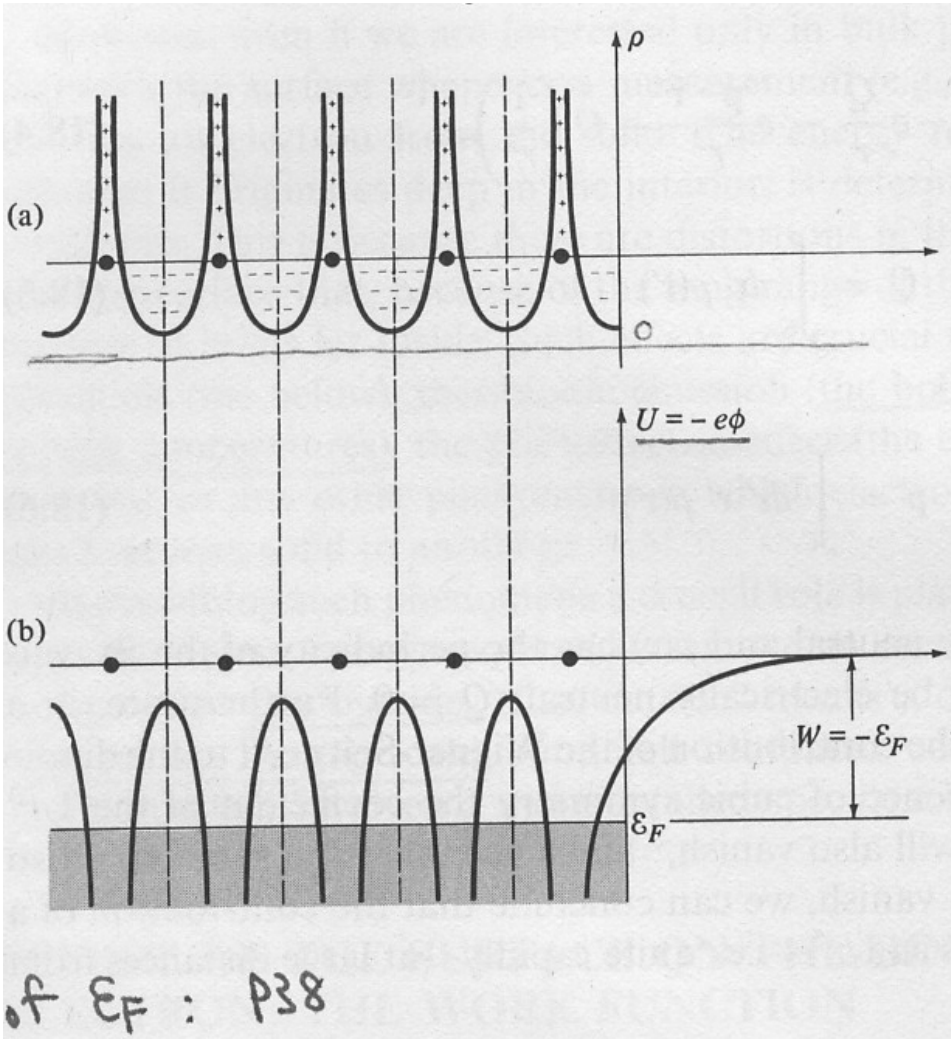

Figure 18.1
(a) The electric charge density near the surface of a finite crystal if there were no distortion in cells near the surface. The density is plotted along a line of ions. Vertical dashed lines indicate cell boundaries. (b) The form of the crystal potential U (or the electrostatic potential $\phi = -U/e$) determined by the charge density in (a), along the same line. Far from the crystal U and ϕ drop to zero. The (negative) Fermi energy is indicated on the vertical axis. The shading below the Fermi energy is meant to suggest the filled electronic levels in the metal. Since the lowest electronic levels outside the metal have zero energy, an energy $W = -\varepsilon_F$ must be supplied to remove an electron.

Ashcroft, Solid State Physics

Double Layer – Work Function

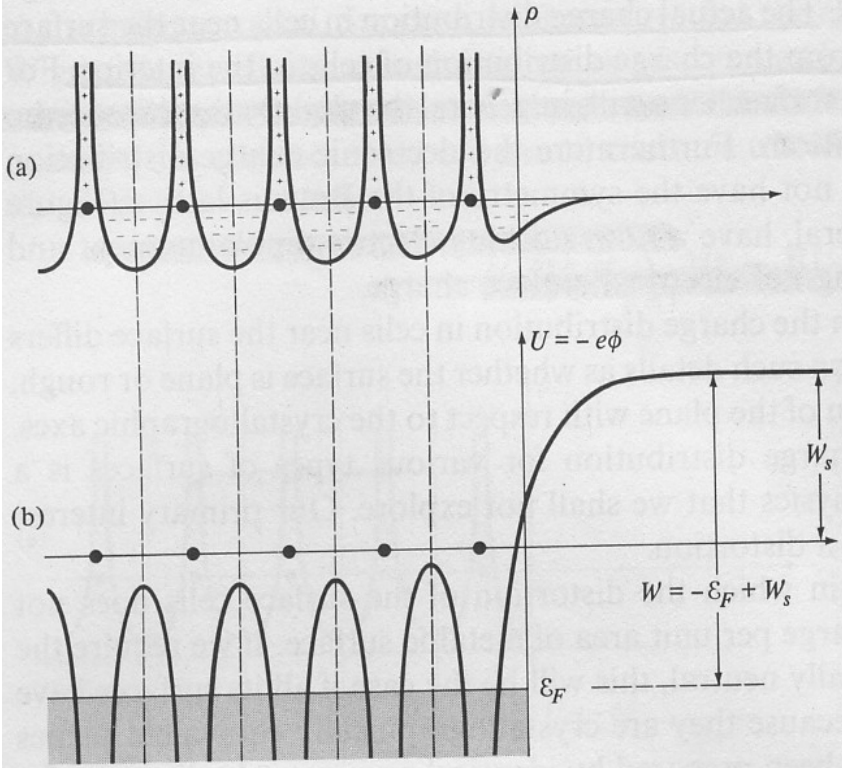

Figure 18.2
(a) The actual form of the electric charge density near the surface of a crystal (neglecting possible slight displacements of the ions near the surface from their sites in the infinite crystal). Note the electron deficiency in the two cells nearest the surface and the presence of electronic charge in the first "cell" on the vacuum side of the surface. It is this kind of distortion that produces the "double layer" described below. (b) The form of the crystal potential U determined by the charge density in (a). If the additive constant is chosen so that U resembles the potential of Fig. 18.1b far inside the crystal, then outside of the crystal U will not approach zero, but the value W_s equal to the work that must be done to carry an electron through the electric field in the double layer. The lowest levels outside the crystal now have an energy W_s, and therefore an energy $W = -\mathcal{E}_F + W_s$ must be supplied to remove an electron.

Ashcroft, Solid State Physics

Potential Profile Across the Double Layer

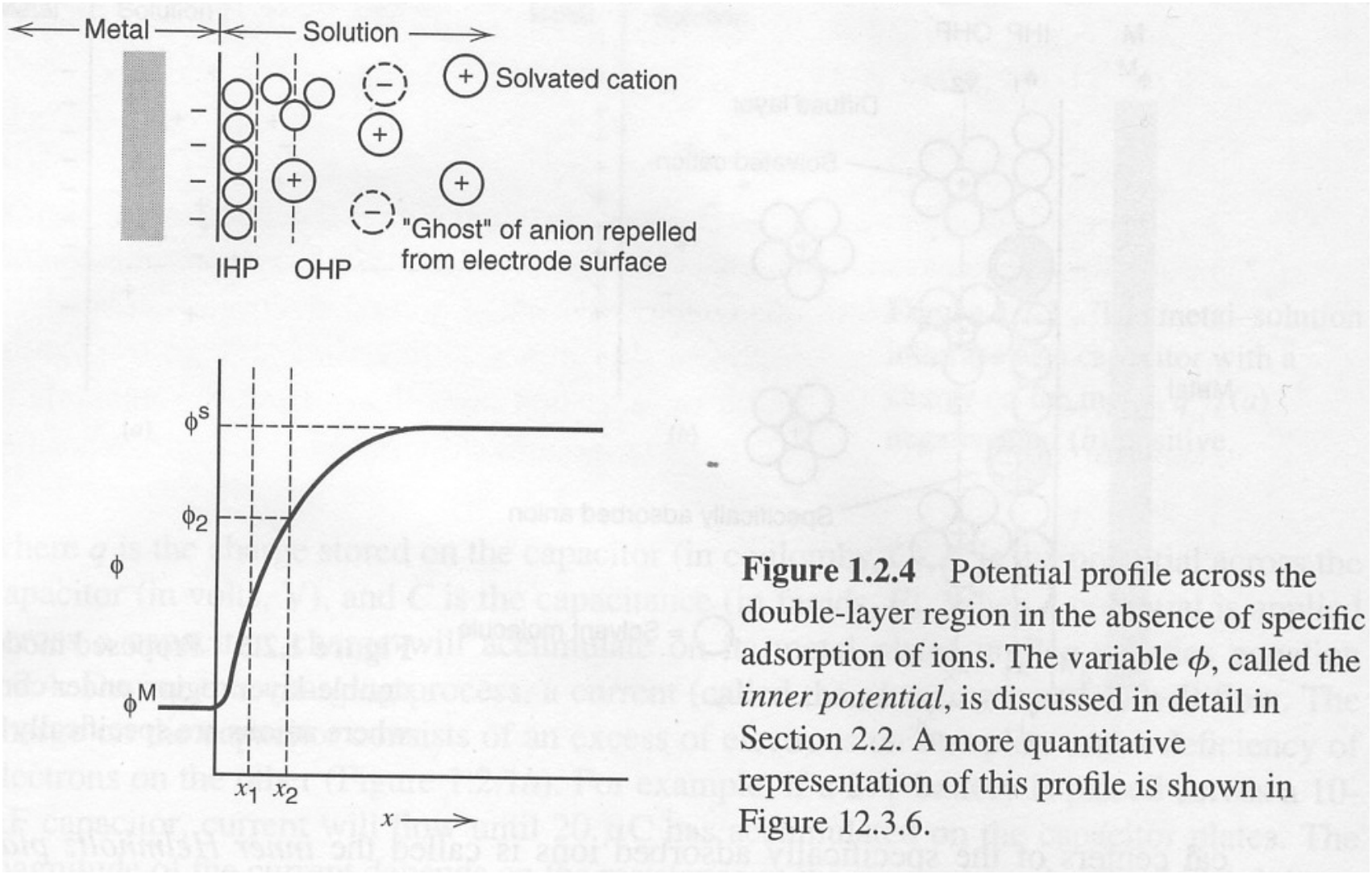

Figure 1.2.4 Potential profile across the double-layer region in the absence of specific adsorption of ions. The variable ϕ, called the *inner potential*, is discussed in detail in Section 2.2. A more quantitative representation of this profile is shown in Figure 12.3.6.

Bard, Electrochemical Methods

Helmholtz Layer and Diffuse Layer

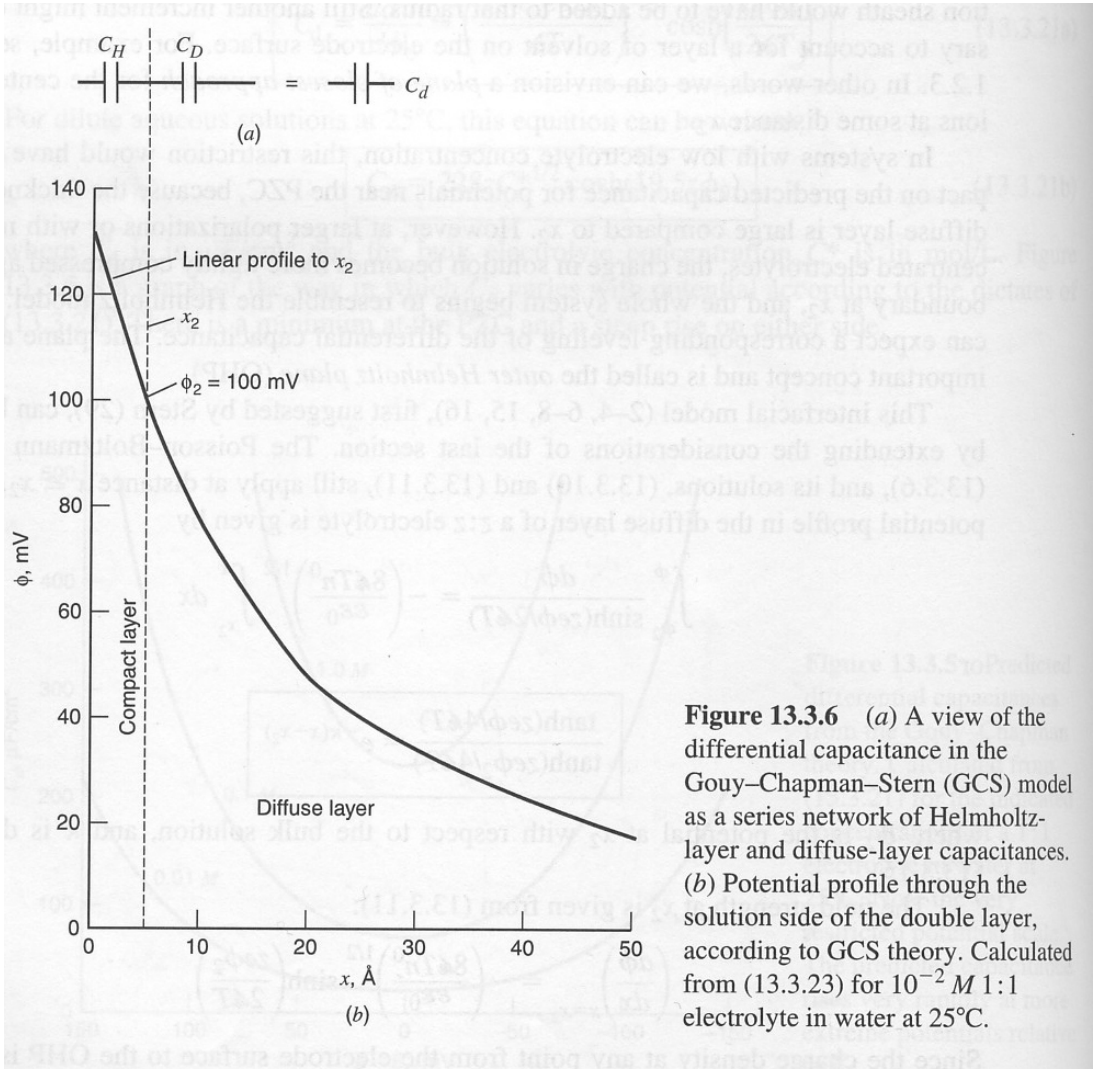

Figure 13.3.6 (*a*) A view of the differential capacitance in the Gouy–Chapman–Stern (GCS) model as a series network of Helmholtz-layer and diffuse-layer capacitances. (*b*) Potential profile through the solution side of the double layer, according to GCS theory. Calculated from (13.3.23) for 10^{-2} *M* 1:1 electrolyte in water at 25°C.

Bard, Electrochemical Methods

Standard Electrode Potentials

TABLE C.1 Selected Standard Electrode Potentials in Aqueous Solutions at 25°C in V *vs.* NHE[a]

Reaction	Potential, V
$Ag^+ + e \rightleftarrows Ag$	0.7991
$AgBr + e \rightleftarrows Ag + Br^-$	0.0711
$AgCl + e \rightleftarrows Ag + Cl^-$	0.2223
$AgI + e \rightleftarrows Ag + I^-$	−0.1522
$Ag_2O + H_2O + 2e \rightleftarrows 2Ag + 2OH^-$	0.342
$Al^{3+} + 3e \rightleftarrows Al$	−1.676
$Au^+ + e \rightleftarrows Au$	1.83
$Au^{3+} + 2e \rightleftarrows Au^+$	1.36
p-benzoquinone $+ 2H^+ + 2e \rightleftarrows$ hydroquinone	0.6992
$Br_2(aq) + 2e \rightleftarrows 2Br^-$	1.0874
$Ca^{2+} + 2e \rightleftarrows Ca$	−2.84
$Cd^{2+} + 2e \rightleftarrows Cd$	−0.4025
$Cd^{2+} + 2e \rightleftarrows Cd(Hg)$	−0.3515
$Ce^{4+} + e \rightleftarrows Ce^{3+}$	1.72
$Cl_2(g) + 2e \rightleftarrows 2Cl^-$	1.3583
$HClO + H^+ + e \rightleftarrows \frac{1}{2}Cl_2 + H_2O$	1.630
$Co^{2+} + 2e \rightleftarrows Co$	−0.277
$Co^{3+} + e \rightleftarrows Co^{2+}$	1.92
$Cr^{2+} + 2e \rightleftarrows Cr$	−0.90
$Cr^{3+} + e \rightleftarrows Cr^{2+}$	−0.424
$Cr_2O_7^{2-} + 14H^+ + 6e \rightleftarrows 2Cr^{3+} + 7H_2O$	1.36
$Cu^+ + e \rightleftarrows Cu$	0.520
$Cu^{2+} + 2CN^- + e \rightleftarrows Cu(CN)_2^-$	1.12
$Cu^{2+} + e \rightleftarrows Cu^+$	0.159
$Cu^{2+} + 2e \rightleftarrows Cu$	0.340
$Cu^{2+} + 2e \rightleftarrows Cu(Hg)$	0.345
$Eu^{3+} + e \rightleftarrows Eu^{2+}$	−0.35
$1/2F_2 + H^+ + e \rightleftarrows HF$	3.053
$Fe^{2+} + 2e \rightleftarrows Fe$	−0.44
$Fe^{3+} + e \rightleftarrows Fe^{2+}$	0.771
$Fe(CN)_6^{3-} + e \rightleftarrows Fe(CN)_6^{4-}$	0.3610

(*continued*)

Bard, Electrochemical Methods (Appendix)

- 2010-09-15